MAPS FOR THE DANGVAN FATIGUE LIMIT IN ROLLING CONTACT FATIGUE

M. Ciavarella[1], F. Monno[2] and G. Demelio[2]

[1]DIASS, Politecnico di BARI, Taranto (Italy)
[2]DIMeG, Politecnico di BARI, BARI (Italy)
E-mail: mciava@poliba.it, filippomonno@libero.it, demelio@poliba.it

ABSTRACT
Recently, various methods have been proposed to assess the risk of Rolling Contact Fatigue failure by Ekberg, Kabo and Andersson, and in particular, the Dang Van multiaxial fatigue criterion has been suggested in a simple approximate formulation. In a recent note by Ciavarella and Maitournam, it was found that the approximation implied can be very significant. Here, a much larger range of conditions is given, partial slip conditions are considered and analytical formulae are also derived.

1. INTRODUCTION
Rolling Contact Fatigue (RCF) occurs in railways, but also in gears and rolling bearings, and many other mechanical applications. It has various forms (plastic deformations, macro- and micro-pitting, spalling, crack initiation from inclusions, etc.) and is generally interacting with other forms of surface damage, and in particular wear. Recently, Ekberg, Kabo and Andersson [1], EKA in the following, have suggested three independent indexes: the first (surface-initiated fatigue) derives from the classical approach based on plasticity theory, shakedown and ratchetting, as described for example in Johnson's book ([2], Ch.9), and hence requires an understanding of material properties related to (cyclic) yield and ratcheting, but even though advanced FEM plasticity models can quite efficiently steady state responses (if there is one) directly [3,4], the ratchetting response modelling remains today one of the most complex in plasticity theory, and even the classical results by Johnson have recently found to be wrong [5,6,7]. Indeed, according to Dang Van [8], even if fatigue limit may be shakedown at grain, so called "mesoscopic", level, fatigue properties of materials are generally directly measured from experiments, rather than extrapolated from plasticity constants which perhaps would be a lot faster and cheaper to obtain. Hence, Dang Van's criterion uses shakedown theories only to evaluate the effect of multiaxiality of the stress cycle by making assumptions on the relationship between macroscopic and microscopic stresses.

As a second criterion, EKA suggest considering for subsurface initiated fatigue a very simple approximate calculation of the Dang Van criterion, and they show that in pure rolling, in the absence of residual stresses, does not depend greatly on the hydrostatic pressure term, and obtained their eq. (11), $\sigma_{eq} = \dfrac{\tau_{\max}}{2}$. Applying this result for the 2D pure rolling problem for which $\tau_{\max} = 0.3 p_0$ ([2], 4.47), where p_0 is the Hertzian peak pressure, and this would give

$\left(p_0 / \tau_e\right)_{\text{lim}} \approx 2 / 0.3 = 6.67$, where τ_e is the endurance limit under pure shear (torsion). If we consider the in-plane shear stress, then $\tau_{\text{max}} = 0.25 p_0$ and $\left(p_0 / \tau_e\right)_{\text{lim}} \approx 2 / 0.25 = 8$. A detailed calculation considering the full 3D state of stress in the plane strain problem and the full DangVan criterion, using Poisson's ratio 0.3, has been completed in [9]. Their Fig.1 shows the results for the line contact problem using the frictionless stress distribution of the Hertz solution [2], as a function of the material constant a_{DV}, varying between 0 (when $\sigma_e / \tau_e = 2$) and 1.5 (when $\sigma_e / \tau_e = 1$). It is found that, contrary to what was suggested by EKA, there is a significant effect of the DangVan constant a_{DV} (i.e. of the hydrostatic component) since the obtained range of limit is $\left(p_0 / \tau_e\right)_{\text{lim}} \approx 4 - 9.2$. The effect of frictional tractions is considered, in full sliding. EKA suggest adding a quadratic decay of the limit with the friction coefficient, but again this is found to be a strong and inaccurate approximation. It appears that very hard material resists a lot better under pure compressive (frictionless) rolling, than under frictional rolling (where there are tensile stresses). This is not particularly surprising, and qualitatively in agreement with gears design standard such as BS ISO 6336-2 [10] or ANSI/AGMA 2001-B88 [11] for pitting resistance of gears, for which materials such as gray cast iron have a lot higher value of recommended pressure than bending stress. The typical ratio between pitting fatigue limit pressure and uniaxial bending fatigue limit varies between 1.5 and 5-6, and therefore although the design practice evidently takes account of many factors and is essentially empirical, the ratio seems to be of the same order of magnitude as the Dang Van criterion applied here.

In the present paper, a larger range of conditions is considered than in [9]. Firstly, the full range of Poisson's ratio is considered in pure rolling, then the entire range of partial slip conditions using Carter's solution and finally, some analytical formulae are derived.

2. DANG VAN ALGORITHM

According to Melan's theorem if a system will shakedown, a time-invariant residual stress tensor must exist, that, together with elastic stresses due to the load, gives a resulting state of stress under the elastic limit. If one can estimate this residual stress tensor $\overline{\rho}$, the state of stress $\overline{\sigma}_k$ (microscopic state of stress) can be calculated as

$$\overline{\sigma}_k = \overline{\Sigma}_k + \overline{\rho} \tag{1}$$

being $\overline{\Sigma}_k$ the bulk stress tensor, and k the k-th time step. If we decompose both stress states into hydrostatic and deviatoric terms

$$\overline{\sigma}_k = \overline{p}_k + \overline{s}_k \tag{2}$$

$$\overline{\Sigma}_k = \overline{P}_k + \overline{S}_k \tag{3}$$

where $\overline{p}_k, \overline{P}_k$ are the hydrostatic terms, and $\overline{s}_k, \overline{S}_k$ the deviatoric ones, and if we consider $\overline{p}_k = \overline{P}_k$, because yielding is affected by deviatoric terms only, equation (1) can be written as

$$\overline{s}_k = \overline{S}_k + dev(\overline{\rho}) \tag{4}$$

Von Mises' yield criterion is adopted for the microscopic stresses:

$$J_2(\overline{s}_k) = \left[\frac{1}{2} \cdot \left(s_{xx}^2 + s_{yy}^2 + s_{zz}^2\right) + s_{xy}^2 + s_{yz}^2 + s_{xz}^2\right]_k \leq K^2 \tag{5}$$

being K the "yield stress" of the given material at microscopic level. This condition makes it possible to find numerically the deviatoric residual stress tensor, because in a six dimensional space with axes $\frac{S_{xx}}{\sqrt{2}}, \frac{S_{yy}}{\sqrt{2}}, \frac{S_{zz}}{\sqrt{2}}, S_{xy}, S_{yz}, S_{xz}$ eq.(5) represents the smallest hypersphere circumscribing the entire load path, centred at $-dev(\overline{\rho})$, as can be inferred substituting eq.(4) in eq.(5). The algorithm is the following:

1. Divide the load path into N discrete time steps, with suitably large N.
2. An initial value for $-dev(\overline{\rho})$ is chosen; the centroid of load path is appropriate: $-dev(\overline{\rho}_0) = \frac{1}{N} \cdot \sum_{k=1}^{N} \overline{S}_k$.
3. Choose an initial small value R_0 for the radius of the hypersphere, for example $R_0 = 0.01$.
4. Calculate the distance of the point $\overline{S}_k$ in the load path from the centre $-dev(\overline{\rho}_{k-1})$, that is to say calculate the radius of the hypersphere on which the point $\overline{s}_k$ lies: $J_2(\overline{s}_k) = J_2(\overline{S}_k + dev(\overline{\rho}_{k-1}))$.
5. Verify that $\overline{S}_k$ lies within the hypersphere: $J_2(\overline{S}_k + dev(\overline{\rho}_{k-1})) - R_{k-1} \leq 0.0$. If it is so, radius and centre of hypersphere rest unchanged and go to step 8; otherwise go to step 6.
6. Increase radius: $R_k = R_{k-1} + \chi \cdot J_2(\overline{S}_k + dev(\overline{\rho}_{k-1}))$, a suitable value for χ is 0.05.
7. Move the centre of the hypersphere so that the point $\overline{S}_k$ lies on the surface of the enlarged hypersphere:
$$-dev(\overline{\rho}_k) = -dev(\overline{\rho}_{k-1}) + \frac{J_2(\overline{S}_k + dev(\overline{\rho}_{k-1})) - R_{k-1}}{J_2(\overline{S}_k + dev(\overline{\rho}_{k-1}))} \cdot (\overline{S}_k + dev(\overline{\rho}_{k-1})).$$
8. Go to the next load point, k=k+1; go to step 4.

When all load points have been analysed, a second loop takes place on the whole load cycle, starting from step 4, and using as initial values for the radius and the centre the last ones obtained from the first loop. Iterations go on till the centre of the hypersphere rests unchanged on the entire load cycle, i.e. its variation is smaller than a prefixed tolerance, for example 10^{-5}. Dang Van's criterion can then be written as follows:

$$\sigma_{eqv}(\overline{s}_k) = \tau_{max}(\overline{s}_k) + \alpha \cdot p(\overline{s}_k) \leq \tau_e \qquad (6)$$

with $\tau_{max}(\overline{s}_k) = \frac{s_{1k} - s_{3k}}{2}$ and $\alpha = 3 \cdot \left(\frac{\tau_e}{\sigma_e} - \frac{1}{2} \right)$, and s_{1k} and s_{3k} are the maximum and minimum principal stress of $\overline{s}_k$ respectively, σ_e, τ_e are the fatigue amplitude limits under pure bending and pure torsion for a given material. When condition in eq.(6) is not respected, a fatigue crack will nucleate under cyclical load.

3. FREE ROLLING

Free rolling about the y axis of a cylindrical body induces the plane strain Hertzian stress field in xz, which has the form:

$$\overline{\overline{\Sigma}} = \begin{pmatrix} \sigma_x & 0 & \tau_{xz} \\ \cdot & \nu \cdot (\sigma_x + \sigma_z) & 0 \\ \cdot & \cdot & \sigma_z \end{pmatrix} \tag{7}$$

The stress cycle is evaluated as variation in the rolling motion of x/a coordinate varying between -5 and 5, with 200 subdivisions, and z/a between 0 and 1, with 150 subdivisions; a is the half width of contact area. At the interface Hertzian pressure distribution

$$p = p_0 \cdot \sqrt{\left[1 - \left(\frac{x}{a}\right)^2\right]}, -1 \le \frac{x}{a} \le 1 \tag{8}$$

all all stresses are normalized with p_0.
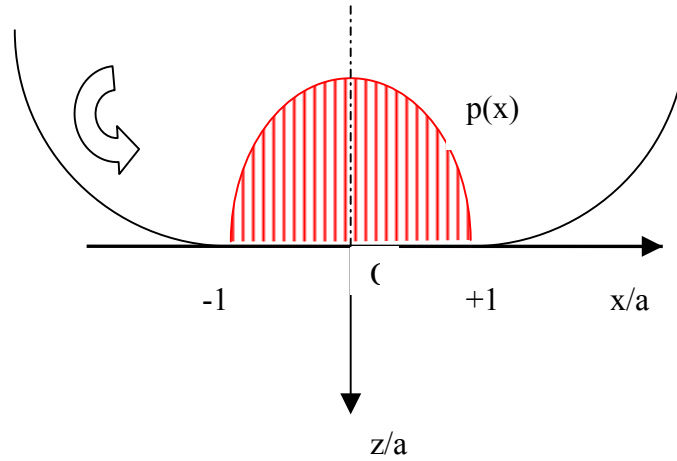
Figure 1: Coordinate system for the rolling problem.

According to eq.(6), at the fatigue limit

$$\max_{k=1,2,\dots N} \left(\frac{p_0}{\sigma_{eqv}(\overline{s}_k)}\right) = \frac{p_0}{\tau_e} \tag{9}$$

Naturally, this calculation is repeated for all possible depths and the limit cycle is found when the highest of all eq.9 is found. This paper will show some results on the fatigue limit ratio $\frac{p_0}{\tau_e}$ as a function of material properties, i.e. Poisson's ratio ν and constant α. Fig 2 shows the fatigue limit ratio for free rolling and the depth where the most severe cycle is localized.
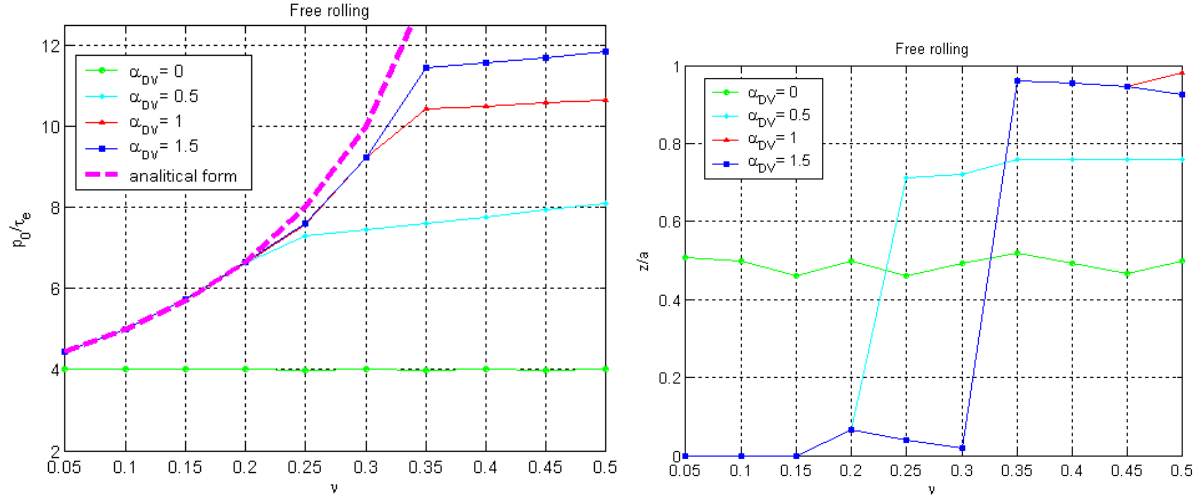
Figure 2: The fatigue limit ratio for free rolling and location of the limit cycle, and comparison with analytical equation (15).

For α =0.0, the limit ratio is 4, and the mean depth is 0.5, independently from Poisson's ratio. The damage is caused by microscopic maximum shear stress only, hydrostatic stress does not give any beneficial contribution, and the maximum of $\dfrac{\tau_{max}(\bar{s})}{p_0}$ is localized at $\dfrac{x}{a} = \mp 0.85$ (see Fig.3) and it is equal to the maximum shear stress $\dfrac{\tau_{xz}}{p_0} = 0.25$. A good analytical form for this case is $\left(\dfrac{p_0}{\tau_e}\right)_{approx} = \left[\max\left(\dfrac{\tau_{xz}}{p_0}\right)\right]^{-1}$. When α > 0.0, the limit ratio $\dfrac{p_0}{\tau_e}$ is strongly affected by the beneficial presence of hydrostatic component. For large enough α, the most severe cycles are on the surface, so the following considerations can be carried out. The surface state of stress is represented by this stress tensor:

$$\bar{\Sigma}_k = \begin{pmatrix} \sigma_x(x_k) & 0 & 0 \\ \cdot & v \cdot (\sigma_x(x_k) + \sigma_z(x_k)) & 0 \\ \cdot & \cdot & \sigma_z(x_k) \end{pmatrix} \tag{10}$$

where

$$\sigma_x(x_k) = \sigma_z(x_k) = -p_0 \cdot \sqrt{1 - \left(\frac{x_k}{a}\right)^2}, -1 \le \frac{x_k}{a} \le 1$$

$$\sigma_x(x_k) = \sigma_z(x_k) = 0.0, \left|\frac{x_k}{a}\right| \ge 1.$$

$$\frac{\sigma_{hyd}(x_k)}{p_0} = -\frac{2}{3} \cdot (1+v) \cdot \sqrt{1 - \left(\frac{x_k}{a}\right)^2} \tag{11}$$

and the normalized deviatoric tensor

$$
\begin{pmatrix}
\dfrac{2\cdot v-1}{3}\cdot\sqrt{1-\left(\dfrac{x_k}{a}\right)^2} & 0 & 0 \\[2ex]
\cdot & \dfrac{2\cdot(1-2\cdot v)}{3}\cdot\sqrt{1-\left(\dfrac{x_k}{a}\right)^2} & 0 \\[2ex]
\cdot & \cdot & \dfrac{2\cdot v-1}{3}\cdot\sqrt{1-\left(\dfrac{x_k}{a}\right)^2}
\end{pmatrix}
\tag{12}
$$

By the substitution $t=\sqrt{1-\left(\dfrac{x_k}{a}\right)^2}$,when $\left|\dfrac{x_k}{a}\right|\le 1$, this represents a line in the three dimensional space, that is the load path in the deviatoric form. The centre of the minimum sphere encompassing the load path is easy to find, because it is the medium point:

$$
\rho_1=\frac{2\cdot v-1}{6},\rho_2=\frac{1-2\cdot v}{3},\rho_3=\frac{2\cdot v-1}{6}
\tag{13}
$$

Microscopic tensions result from the difference of the corresponding components of (12,13) respectively. The maximum ratio of peak Hertzian pressure and τ_e is reached at $\dfrac{x_k}{a}=\mp 1$, due to the symmetry of load history. So the microscopic stresses are obtained taking $t=0$:

$$
s_1=s_3=\frac{1-2\cdot v}{6}\ge 0, s_2=\frac{2\cdot v-1}{3}\le 0
\tag{14}
$$

The microscopic maximum shear stress is $\tau_{\max}(\bar s)=\dfrac{s_1-s_2}{2}=\dfrac{1-2\cdot v}{4}$, the hydrostatic tension is $\sigma_{hyd}(\bar s)=-\dfrac{2}{3}\cdot(1+v)\cdot t=0.0$, and the approximate fatigue limit ratio is

$$
\left(\frac{p_0}{\tau_e}\right)_{approx}=\left[\frac{1-2\cdot v}{4}\right]^{-1}
\tag{15}
$$

which is independent from the material constant α.
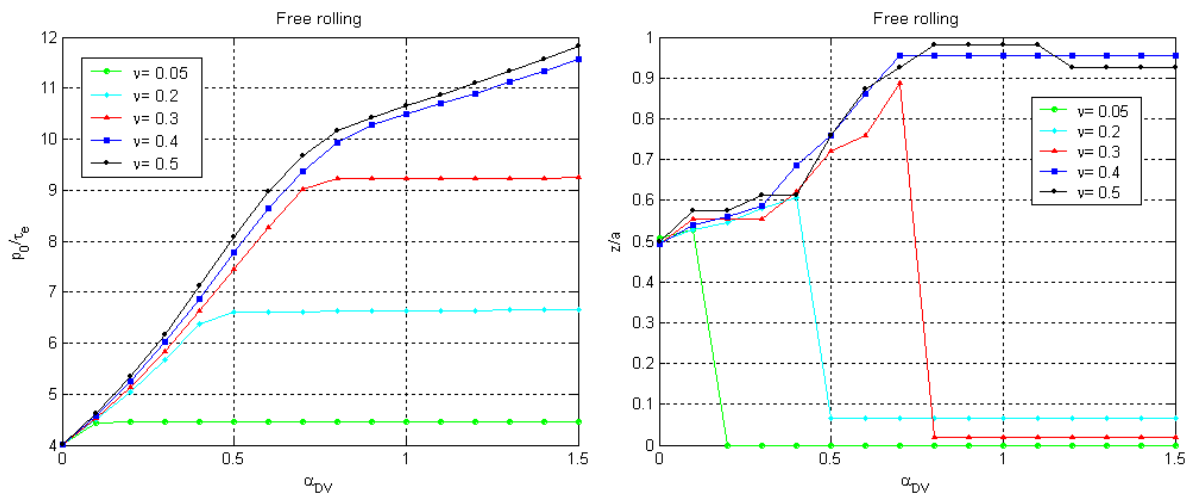
Figure 3: The fatigue limit ratio for free rolling and location of the limit cycle, as in Fig.2, but with different choice of x axis.

The approximation is good up to $\nu = 0.2$ better for large α. In figure 3, the variation of fatigue limit ratio and the corresponding depth with α are plotted.

4 . TRACTIVE ROLLING

Frictional rolling contact for cylindrical bodies is plane strain is given by Carter's solution (see Johnson, 1985), given by the superposition of stresses due to Hertzian pressure and tangential tractions on the surface. These are calculated by a linear combination of surface tangential tractions in the sliding contact problem:

$$q(x) = q'(x) + q''(x)$$

$$q'(x) = \mu \cdot p_0 \cdot \sqrt{1 - \left(\frac{x}{a}\right)^2} \tag{16}$$

$$q''(x) = -\frac{c}{a} \cdot \mu \cdot p_0 \cdot \sqrt{1 - \left(\frac{x+d}{c}\right)^2}$$

where d is the offset from the centre toward the leading edge of the contact area, and it is related to c:

$$\frac{d}{a} = 1 - \frac{c}{a} = 1 - \sqrt{1 - \frac{Q_x}{\mu \cdot P}} \tag{17}$$

being Q_x and P the resultants of surface tangential tractions along x axis and Hertzian pressure, respectively, and μ the friction coefficient. With the same grid of points of the frictionless problem, graphs of $\frac{p_0}{\tau_e}$ are plotted, taking into account two more parameters:

$\frac{Q_x}{\mu \cdot P}$ and μ. The following figures show $\frac{p_0}{\tau_e}$ versus μ for different α and the depths of the most severe cycles; only some values for ν and $\frac{Q_x}{\mu \cdot P}$ are considered, for space limitations.
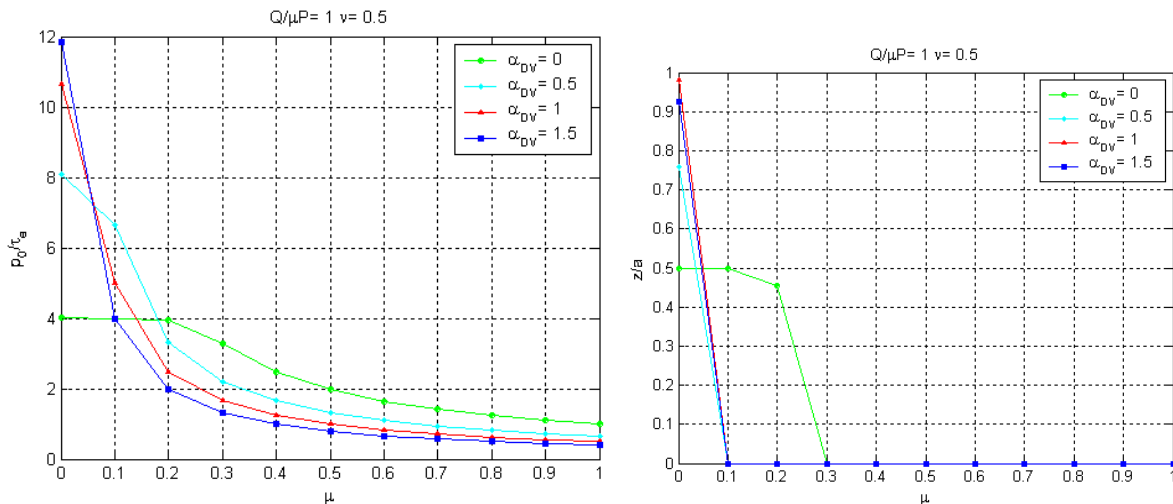
Figure 4: The fatigue limit ratio in full sliding ($\frac{Q_x}{\mu \cdot P}$ =1) and location of limit cycle, ν=0.5.
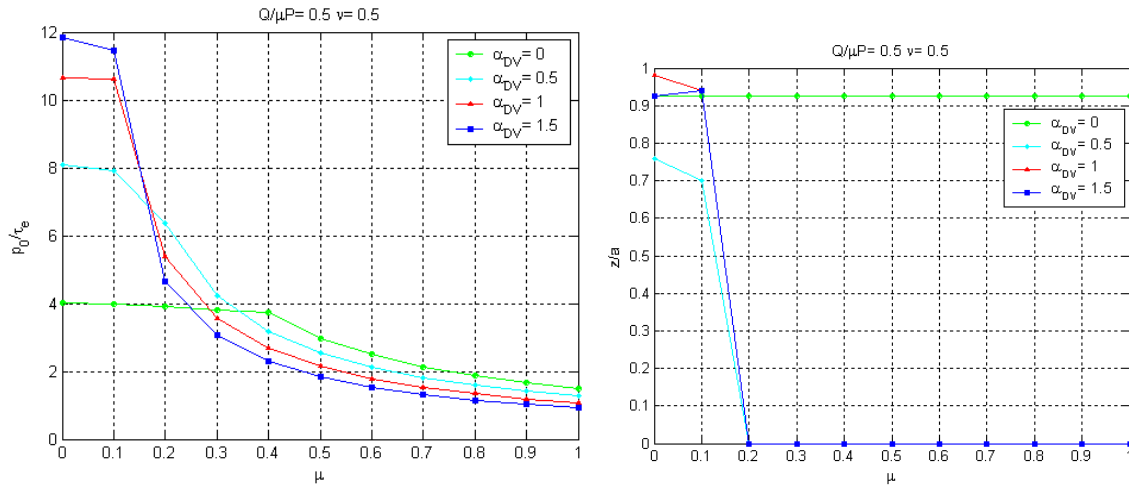
Figure 5: The fatigue limit ratio in partial slip ($\frac{Q_x}{\mu \cdot P}$ =0.5) and location of limit cycle, ν=0.5.
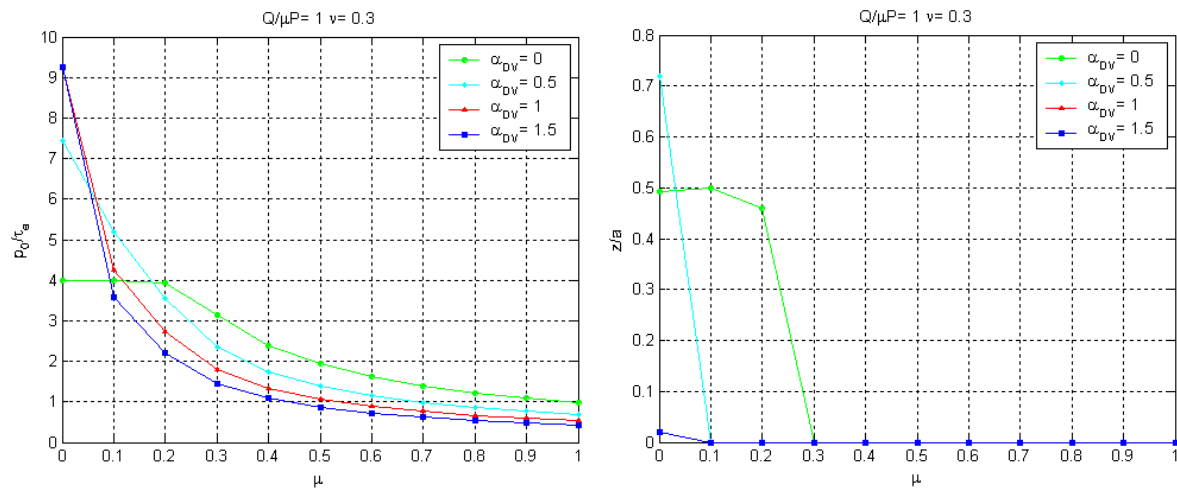
Figure 5: The fatigue limit ratio in full slip ($\frac{Q_x}{\mu \cdot P}$ =1) and location of limit cycle, ν=0.3.
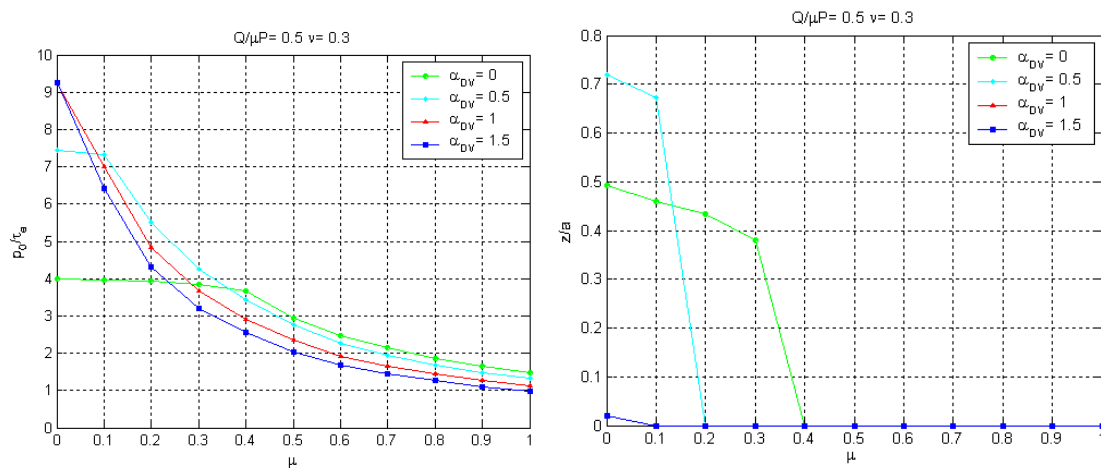
Figure 6: The fatigue limit ratio in partial slip ($\frac{Q_x}{\mu \cdot P}$ =0.5) and location of limit cycle, ν=0.3.

For sufficiently large friction and Dang Van's constant, the fatigue limit is reached on surface, and the highest $\sigma_{eqv}(\overline{s}_k)$, according to Dang Van's criterion, is at $x/a = -1$, where the biaxial state of stress is:

$$\sigma_x(\frac{x}{a} = -1) = \sigma'_x(\frac{x}{a} = -1) + \sigma''_x(\frac{x}{a} = -1)$$

$$\sigma'_x(\frac{x}{a} = -1) = -p_0 \cdot \left(\sqrt{1-(-1)^2} + 2 \cdot \mu \cdot (-1)\right) \quad (18)$$

$$\sigma''_x(\frac{x}{a} = -1) = \frac{c}{a} \cdot p_0 \cdot \left(\sqrt{1 - \left(\frac{-1+\frac{d}{a}}{\frac{c}{a}}\right)^2} + 2 \cdot \mu \cdot \left(\frac{-1+\frac{d}{a}}{\frac{c}{a}}\right)\right)$$

and

$$\sigma_x(\frac{x}{a} = -1) = 2 \cdot \mu \cdot p_0 \cdot \left(1 - \sqrt{1 - \frac{Q_x}{\mu \cdot P}}\right) ;$$

$$\tau_{xz}(\frac{x}{a} = -1) = \tau'_{xz}(\frac{x}{a} = -1) + \tau''_{xz}(\frac{x}{a} = -1)$$

$$\tau'_{xz}(\frac{x}{a} = -1) = -\mu \cdot p_0 \cdot \sqrt{1-(-1)^2} \quad (19)$$

$$\tau''_{xz}(\frac{x}{a} = -1) = -\frac{c}{a} \cdot p_0 \cdot \sqrt{1 - \left(\frac{-1+\frac{d}{a}}{\frac{c}{a}}\right)^2}$$

Hence, $\tau_{xz}(\frac{x}{a} = -1) = 0.0$; $\sigma_z(\frac{x}{a} = -1) = 0.0$, the Hertzian pressure being null on the leading

edge. The hydrostatic tension is $\sigma_{hyd} = \frac{2}{3} \cdot (1+v) \cdot \mu \cdot \left(1 - \sqrt{1 - \frac{Q_x}{\mu \cdot P}}\right)$ \quad (20)

In full slip, $\frac{Q_x}{\mu \cdot P} = 1.0$, there is no significant difference between nominal and microscopic tensions because the residual stress tensor is negligible. Microscopic and nominal maximum shear stress are very similar, so a simplified formulation of fatigue limit pressure can be obtained through the deviatoric part of nominal stress tensor:

$$\begin{pmatrix} 2 \cdot \frac{2-v}{3} \cdot \mu \cdot \left(1 - \sqrt{1 - \frac{Q_x}{\mu \cdot P}}\right) & 0.0 & 0.0 \\ \cdot & 2 \cdot \frac{2 \cdot v - 1}{3} \cdot \mu \cdot \left(1 - \sqrt{1 - \frac{Q_x}{\mu \cdot P}}\right) & 0.0 \\ \cdot & \cdot & -\frac{2}{3} \cdot (1+v) \cdot \mu \cdot \left(1 - \sqrt{1 - \frac{Q_x}{\mu \cdot P}}\right) \end{pmatrix} \quad (21)$$

The maximum shear stress is the semi-difference of the first and the third principal stress:

$$\tau_{max} = \mu \cdot \left(1 - \sqrt{1 - \frac{Q_x}{\mu \cdot P}}\right) \quad (22)$$

The analytical form for full sliding is then

$$\left(\frac{p_0}{\tau_e}\right)_{approx} = \left[\mu \cdot \left(1 - \sqrt{1 - \frac{Q_x}{\mu \cdot P}}\right) \cdot \left(1 + \frac{2}{3} \cdot \alpha \cdot (1+\nu)\right)\right]^{-1} \qquad (23)$$
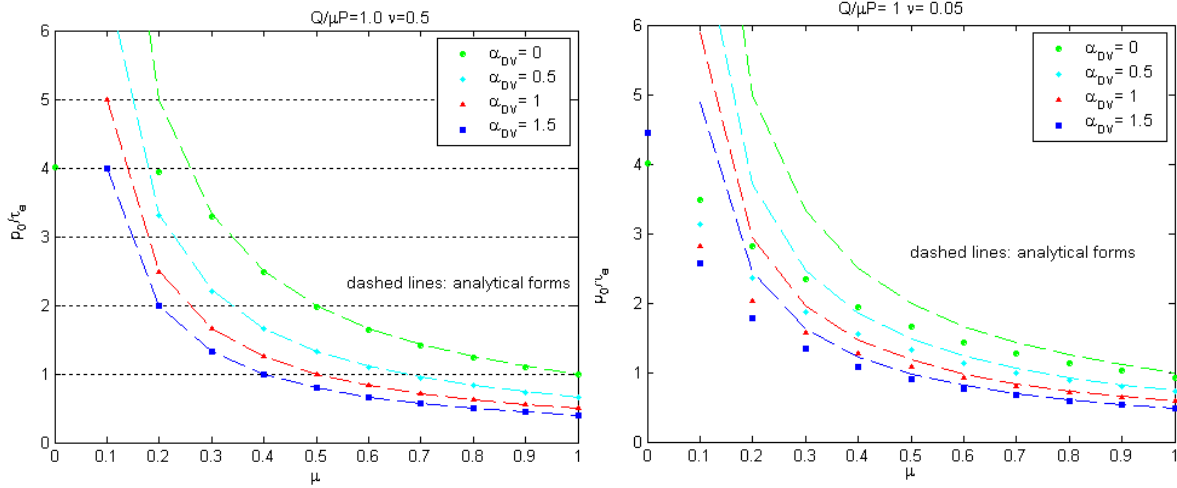
Figure 7: The fatigue limit ratio in full slip ($\frac{Q_x}{\mu \cdot P}$ =1) for ν=0.5 and for ν=0.05.

This equation (23) is seen in Fig.7 to work more efficiently for large ν=0.5 and be poor for small ν=0.5 except at large friction coefficients.

In partial slip the difference between microscopic and nominal stresses is no longer more negligible see Fig.8.
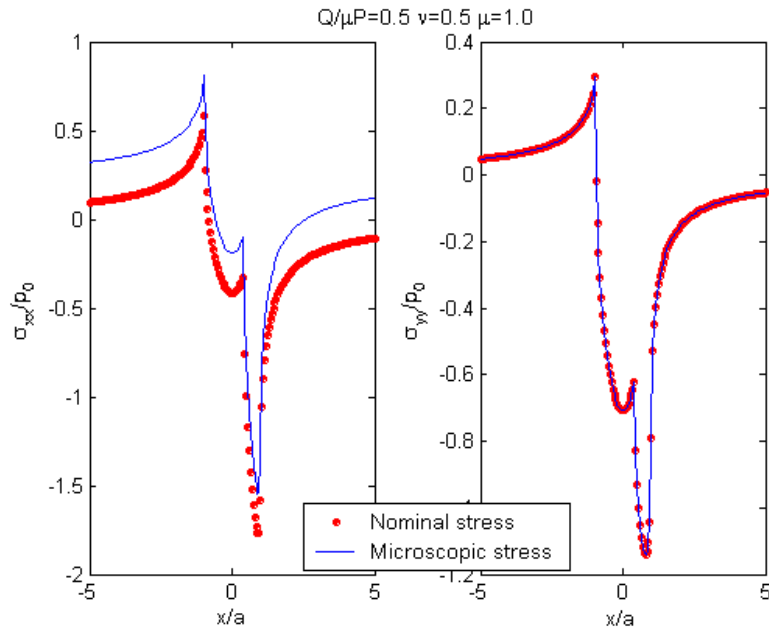
(a)

Figure 8: (Caption on the next page)
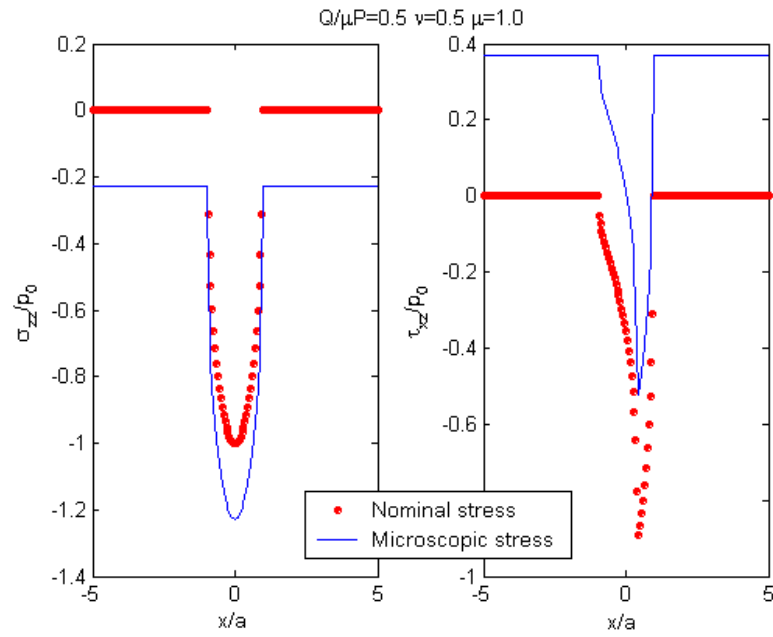
(b)

Figure 8: The stress fields in partial slip ($\frac{Q_x}{\mu \cdot P}$=0.5) for v=0.5 and μ=1

This results in a different maximum shear stress, as seen Fig.9.
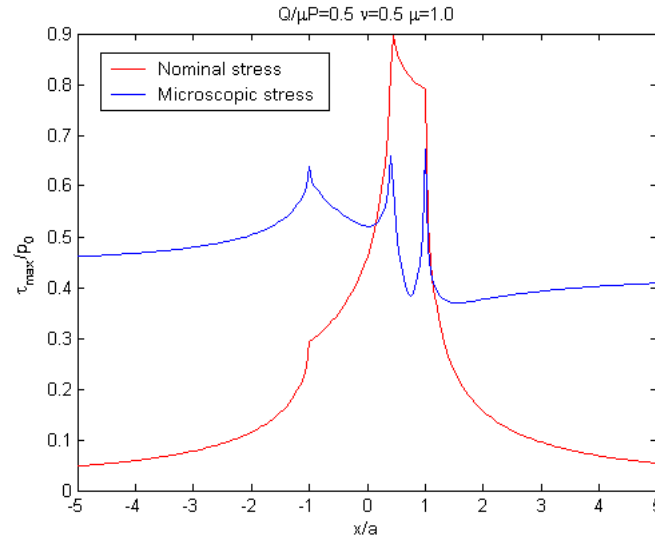
Figure 9: The Tresca stress in partial slip ($\frac{Q_x}{\mu \cdot P}$=0.5) for v=0.5 and μ=1

A simple way to estimate the analytical form in partial slip is to calculate the ratio between microscopic and nominal shear stress for different friction coefficients. For example, for

v=0.5. The mean ratio between microscopic and nominal maximum shear stress is seen to decrease as $\dfrac{1}{\left(\dfrac{Q_x}{\mu \cdot P}\right)}$, roughly, as seen in Fig.10 (at least for high $\dfrac{Q_x}{\mu \cdot P}$).
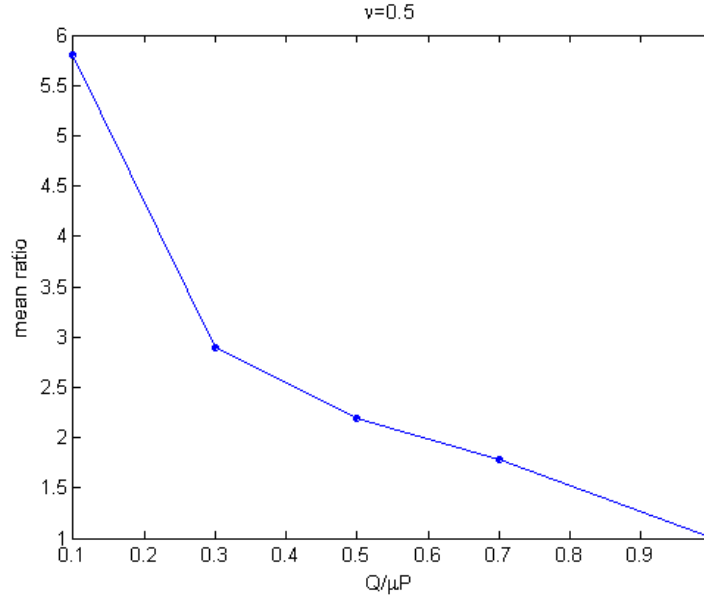
Figure 10: The ratio of Tresca microscopic to nominal stress in partial slip for v=0.5

Hence, the following formulation is suggested, in order to correct the full slip formula (where the ratio is unitary):

$$ratio = \frac{1}{\dfrac{Q_x}{\mu \cdot P}} + v \cdot \sqrt{1 - \frac{Q_x}{\mu \cdot P}} \qquad (24)$$

The analytical form of limit pressure in partial slip is finally obtained as

$$\left(\frac{p_0}{\tau_e}\right)_{approx} = \left[\mu \cdot \left(1 - \sqrt{1 - \frac{Q_x}{\mu \cdot P}}\right) \cdot \left[\left(\frac{1}{\dfrac{Q_x}{\mu \cdot P}} + v \cdot \sqrt{1 - \frac{Q_x}{\mu \cdot P}}\right) + \frac{2}{3} \cdot \alpha \cdot (1+v)\right]\right]^{-1} \qquad (25)$$
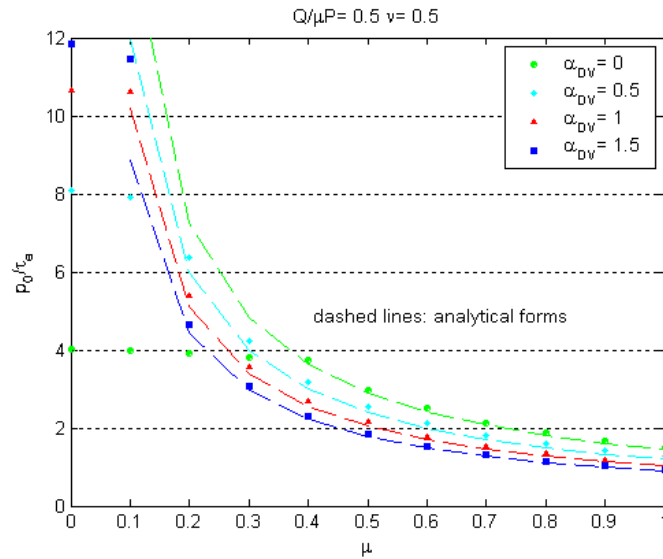
Figure 11: The fatigue limit ratio in partial slip ($\dfrac{Q_x}{\mu \cdot P}$ =0.5) for v=0.5

The numerical results are compared with the analytical formula (25) in the fig.11,12.
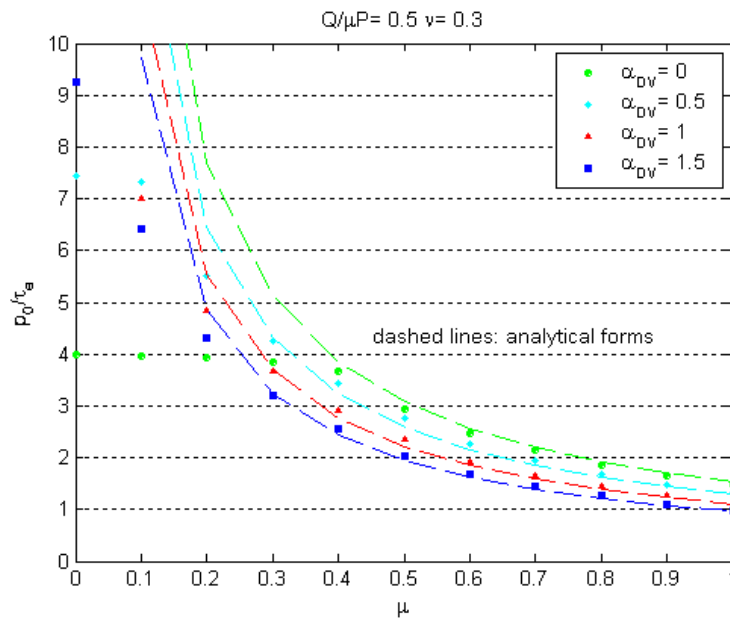
Figure 12: The fatigue limit ratio in partial slip ($\dfrac{Q_x}{\mu \cdot P}$ =0.5) for v=0.3

CONCLUSIONS

The Ekberg, Kabo and Andersson (2002) criterion for fatigue limit using the Dang Van multiaxial fatigue criterion has been corrected and given in much more precise analytical formulation. This will permit to avoid most calculations, at least in 2d problems. A full investigation is now in progress to cover also the 3d case.

References

[1] A. Ekberg, E. Kabo and H. Andersson, (2002) An engineering model for prediction of rolling contact fatigue of railway wheels *Fat Fract Engng Mat & Struct* **25** (10) 899-909

[2] K. L. Johnson, (1985) Contact Mechanics. Cambridge University Press, Cambridge.

[3] K. Dang Van, MH Maitournam, B. Prasil, (1996) Elastoplastic analysis of repeated moving contact - Application to railways damage phenomena *Wear* **196** (1-2): 77-81

[4] N. Maouche N, M.H. Maitournam, K. DangVan (1997) On a new method of evaluation of the inelastic state due to moving contacts *Wear* **203**: 139-147

[5] A.R.S., Ponter, L. Afferrante, and M. Ciavarella, (2002) Shakedown in Rolling Contact. Fatigue 2002 - *Proc. Eighth Int Fat. Congress,* Stockholm, Vol. **2**, ISBN 1901537307, EMAS Cradley Heath (UK), pp. 1355-1363.

[6] A.R.S., Ponter, L. Afferrante, and M. Ciavarella, (2004) A note on Merwin's analysis of forward flow in rolling contact, *Wear* **256**, 3-4, 321-328

[7] L. Afferrante, M. Ciavarella and G. Demelio, (2004), A Re-examination of Rolling Contact Fatigue Experiments by Clayton & Su with Suggestions for Surface Durability Calculations, *Wear* **256 3-4** 329-334.

[8] K. Dang Van, G. Cailletaud, G., J.F. Flavenot, A. Le Douaron, H.P. and Lieurade (1989) Criterion for high cycle fatigue failure under multiaxial loading. In: Biaxial and Multiaxial Fatigue (Ed. by M.W.Brown and K.J.Miller), Mechanical Engineering Publications, London, UK, 459-478

[9] M.Ciavarella, H. Maitournam, (2004) On the Ekberg, Kabo and Andersson calculation of the Dang Van High Cycle Fatigue limit for Rolling Contact Fatigue, Letter to the Editor, Fatigue Fract. Engng. Mater. Struct. **27 (6):** 523-526

[10] BS ISO 6336-2 (1996) Calculation of load capacity of spur and helical gears (Part 2 Calculation of surface durability (pitting); Part 5: Strength and quality of materials).

[11] ANSI/AGMA 2001-B88, (1988) Fundamental rating factors and calculation methods for involute spur and helical gears.